Journal of Power Sources 203 (2012) 126–129

Contents lists available at SciVerse ScienceDirect

Journal of Power Sources

journal homepage: www.elsevier.com/locate/jpowsour

Short communication

"In-operando" neutron scattering studies on Li-ion batteries

A. Senyshyn[a,b,*], M.J. Mühlbauer[a,c], K. Nikolowski[a,e], T. Pirling[d], H. Ehrenberg[a,e,f]

[a] Material Science, Technische Universität Darmstadt, Petersenstrasse 23, D-64287 Darmstadt, Germany
[b] Forschungsneutronenequelle Heinz-Maier Leibnitz FRM-II, Technische Universität München, Lichtenbergstrasse 1, D-85748 Garching b. München, Germany
[c] Physik-Department E21, Technische Universität München, James-Franck-Strasse, D-85748 Garching b. München, Germany
[d] Institut Laue-Langevin, 6 rue Jules Horowitz, Grenoble Cedex 9, BP 156 – 38042, France
[e] Karlsruhe Institute of Technology (KIT), Institute for Applied Materials (IAM), Hermann-von-Helmholtz-Platz 1, D-76344 Eggenstein-Leopoldshafen, Germany
[f] Helmholtz-Institute Ulm for Electrochemical Energy Storage (HIU), P.O. Box 3640, 76021 Karlsruhe, Germany

ARTICLE INFO

Article history:
Received 23 August 2011
Received in revised form 31 October 2011
Accepted 6 December 2011
Available online 14 December 2011

Keywords:
Li-ion battery
In-operando studies
Electrodes
Fatigue
Neutron powder diffraction
Neutron radiography

ABSTRACT

Anode and cathode materials, graphite and $LiCoO_2$, are studied by neutron diffraction under "in operando" conditions in commercial batteries (ICR 18650-type). The evolution of their crystal structure versus state of charge (SOC) and fatigue (state of health, SOH) has been analyzed using the Rietveld refinement technique. Neutron radiography data and their tomography reconstruction revealed the local neutron absorption density, which reflects mainly the Li-distribution density, but also further details of the battery design. Changes in the neutron absorption contrast have also been evaluated in dependence on SOC and SOH.

The lithium-ion batteries are extensively used in diverse power applications, e.g. consumer electronics, communication devices, power tools, etc. It is expected that the Li-ion battery will be the "get round" technology for the electrification of the drivelines as well as for the stationary storage for an effective use of renewable energy sources. Very intensive development and research was achieved in the last decades and its progress can be seen in everyday life. However, the next step is to establish Li-ion batteries as the main energy storage system for electromobility. This requires significant technological progress regarding safety, lifetime, temperature range of stable operation and higher energy and power densities, which calls for further studies to elucidate the underlying processes inside a battery during operation. Another major challenge concerns the safe operation of Li-ion batteries under improper or extreme and "misuse" conditions. The high amount of Li inside a battery in combination with its high reactivity makes the battery very sensitive to the conditions of operation, and its improper use was already reported to be the reason for serious hazards. The high chemical activity of the battery constituents results in a significant materials interaction and the control of possible risks requires a systematic investigation of the Li-ion battery under real operation conditions "*in-operando*".

Neutron scattering is a non-alternative and non-destructive tool for probing of complex lithium containing systems due to peculiar features of neutrons, e.g. the ability to localize light atoms (lithium and oxygen) and to distinguish between different isotopes, the high penetration depth of neutrons and the nearly constant neutron form-factors, independent from momentum transfer. Such features of neutrons make them especially attractive for studies of lithium ion batteries "*in-operando*", but the available information about such studies in the literature is rather limited. To our knowledge only a few attempts have been made to study commercial Li-ion batteries using medium resolution neutron powder diffraction adopting $LiFePO_4$ [1,2], $LiCoO_2$ [3] or $LiMn_2O_4$ [4] cathode along with a few applications of medium resolution neutron radiography [5–8].

In our turn we report "*in-operando*" high-resolution neutron scattering studies on commercial-type Li-ion batteries. Two batteries (namely "fresh" and "fatigued") were taken from the same batch of rechargeable batteries of the cylindrical 18650 type. For testing purposes only single charge/discharge cycle was applied for "fresh" battery after formation, whereas "fatigued" one underwent 200 sequential charges and discharges (3.0–4.2 V, CCCV, 2.6 A discharge current, ambient temperature), which resulted in the reduction of

* Corresponding author at: Forschungsneutronenequelle Heinz-Maier Leibnitz FRM-II, Technische Universität München, Lichtenbergstrasse 1, D-85748 Garching b. München, Germany. Tel.: +49 8928914316; fax: +49 8928914911.
E-mail address: anatoliy.senyshyn@gmail.com (A. Senyshyn).

0378-7753/$ – see front matter © 2011 Elsevier B.V. All rights reserved.
doi:10.1016/j.jpowsour.2011.12.007

discharge capacity from ca. 2 Ah to ca. 1.3 Ah (see Fig. S1) as well as in significant difference in open voltage vs. capacity curves (see Fig. S2). For fatigue purposes the cycling of the cells was controlled by a multichannel potentiostat from BASYTEC©.

Neutron scattering experiments were carried out on both "fresh" and "fatigued" commercial Li-ion cells, and the charge of the cells was controlled by a VMP3 potentiostat from Bio-Logic©. The evolution of the structures of the crystalline battery materials was followed under different states of charge, based on high-resolution neutron powder diffraction experiments, performed on the powder diffractometer SPODI [9].

Experiments were carried out at ambient conditions. Monochromatic neutrons ($\lambda = 1.5481(1)$ Å) were selected at a 155° take-off using the (5 5 1) reflection of a vertically focused composite Ge monochromator. The vertical position-sensitive multidetector (300 mm effective height), consisting of 80 ^{3}He tubes and covering an angular range of 160° 2θ, was used for data collection. Measurements were performed in Debye–Scherrer geometry. Data were recorded "*in-operando*", i.e. the desired charge level was kept constant for 2 h and then allowed to relax. The data collection time per battery was ca. 3.5 h and it was performed at distinguished states of charge: open cell voltage (3.40 for the fresh cell, 3.60 for the fatigued cell), 3.90, 3.95, 4.00, 4.05, 4.10, 4.15 and 4.20 V.

The observed neutron diffraction patterns are characterized by a reasonably high background increasing at high angles, which is very similar for the "fresh" and "fatigued" batteries and does not depend on the state of charge of the battery. Rietveld refinement was applied for the Li_xCoO_2 cathode material, the graphite anode and the current collector materials Al and Cu, while a structure independent (Le Bail) profile fit was performed for the steel housing, using the software package FullProf [10]. The peak profile shape was described by a Thompson–Cox–Hastings pseudo-Voigt function. The instrumental resolution function was determined for a $Na_2Ca_3Al_2F_{14}$ reference material and explicitly used for the calculation of the reflections half widths. Additional peak broadening from the sample was taken into account as phase-specific microstrain or in the case of graphite and the Li-intercalated graphites as a crystallite size effect. The background of the diffraction pattern was fitted using a linear interpolation between selected data points in non-overlapping regions.

Examples of Rietveld refinement for "fresh" battery discharged to 3.40 V and charged to 4.10 V are shown in Fig. 1. Clear signals corresponding to the cathode material Li_xCoO_2, both copper and aluminium current collectors, steel housing as well as graphite anode and lithium intercalated carbons were observed. Charging of the battery introduces significant changes to the structure of components, while on the first view neutron powder diffraction patterns collected for both "fresh" and "fatigued" batteries charged to the same state have been found very similar. Hence, closer look on the results of Rietveld refinement indicates some differences, which occur on both cathode and anode sides. The analysis of the structural evolution occurring on the cathode Li_xCoO_2 side is discussed first.

The best fits to the observed reflections from the cathode Li_xCoO_2 in "fresh" and "fatigued" cells were obtained with the parameters listed in Table S1. The charging of the battery results in Li extraction from the cathode, i.e. a diminution of the Li content with increasing voltage. Furthermore the reduction of lithium content in Li_xCoO_2 causes an increase of lattice parameter *c* and cell volume. This feature is already reported [11] and can be explained in terms of the rhombohedral $LiCoO_2$ layered structure along the [0 0 1] direction (in hexagonal setting), where layers are formed by alternating LiO_6 and CoO_6 octahedra. Upon charging of the battery from 3.4 to 4.2 V the Co–O distance is raised by about 0.03 Å, while Li–O distance is reduced by ca. 0.08 Å. Shortening of *c* lattice parameter as well as Li–O interatomic distance

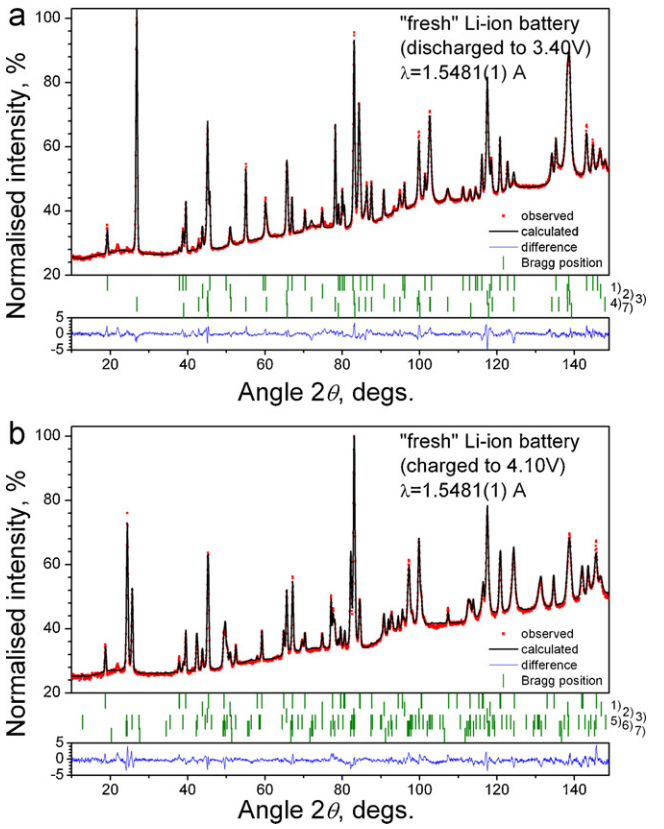

Fig. 1. Rietveld refinement of diffraction pattern from commercial 18650 Li-ion battery ("fresh") discharged to 3.40 V (left) and charged to 4.10 V (right). Experimental data are shown by points, lines denote calculated profiles and lower plots – their difference. Calculated positions of Bragg reflections are shown by vertical tick marks, where rows (1–7) correspond to cathode Li_xCoO_2 (1), copper current collector (2), steel housing (3), anode graphite (4) and lithium intercalated carbons LiC_{12} (5) and LiC_6 (6), aluminium current collector (7).

in $LiCoO_2$ can be understood in terms of van der Waals forces which are typical for Li bonds. Intercalation of lithium results in an increase of lithium content and, as a consequence, in a strengthening of lithium oxygen bonding, which causes shortening of Li–O bonds, *c* lattice parameter and cell volume.

Unfortunately there is a lack of systematic *in situ* structural investigations on $LiCoO_2$ upon Li de/intercalation in the literature. Therefore data from Rodriguez et al. [12] (*ex situ* X-ray powder diffraction studies of Li_xCoO_2 from commercial 18650-type battery, Sony Corp.) were taken for comparison to our data collected for both "fresh" and "fatigued" batteries. Result of such comparison is shown in Fig. 2 by black (diamonds), blue (squares) and red (circles) respectively. Our "*in-operando*" data are in fair agreement with *ex situ* data of Rodriguez et al. [12], but with better detalization, thus giving clear evidence for anomalies in *c* lattice parameter and cell volume occurring in commercial Li-ion cell.

Dependencies of Li_xCoO_2 lattice parameters for both "fresh" and "fatigued" batteries have been found very similar, but at low voltages (and, respectively, at high Li contents) the *c* lattice parameter of "fatigued" cell is little higher than respective one for "fresh" cell. Opposite behaviour has been noticed for *a* lattice parameter, i.e. the cell dimension in the *ab*-plane of the hexagonal lattice is lower for a "fatigued" cell as compared to a "fresh" one. Observed changes in lattice parameters might be related to changes in the lithium content introduced by fatigue.

The occupations on the Li site in Li_xCoO_2 were determined via Rietveld refinement, but are considerably influenced by correlations with other parameters and need to be interpreted with

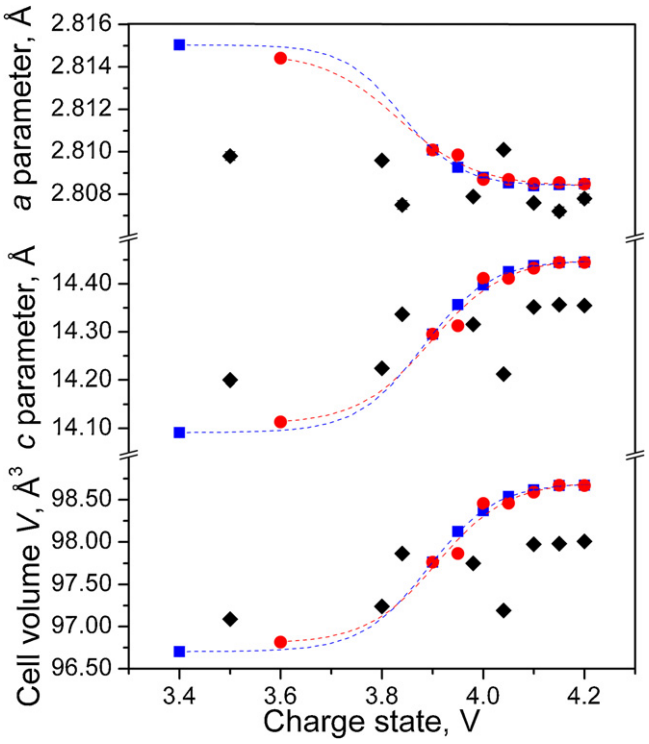

Fig. 2. Lattice parameters and cell volume of Li_xCoO_2 cathode for "fresh" (blue square) and "fatigued" (red circles) Li-ion batteries. *Ex situ* X-ray powder diffraction studies of Li_xCoO_2 from commercial 18650-type battery from Sony Corp. from Rodriguez et al. [12] are shown by black diamonds. Dashed lines are guides for the eyes. (For interpretation of the references to colour in this figure legend, the reader is referred to the web version of the article.)

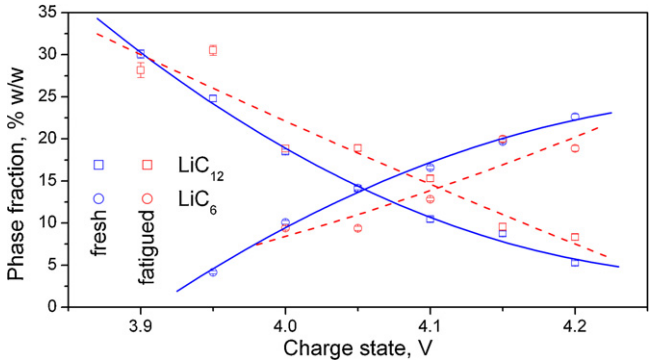

Fig. 3. The relationship of weight fractions for LiC_6 and LiC_{12} as determined from Rietveld refinement for "fresh" and "fatigued" Li-ion batteries.

care (see Table S1). The completely discharged battery should deliver/obey the Li site occupation x_{Li} in Li_xCoO_2 close to one and will be reduced upon charging of the battery. It is known [13,14] that at $x_{Li} \approx 0.5$ Li_xCoO_2 undergoes a transition to a monoclinic structure. Some authors [13–15] also argued that staging (formation of intermediate hexagonal phases with different x_{Li}) would occur in Li_xCoO_2 upon lithium de-/intercalation. The analysis of the obtained diffraction data did neither reveal any traces of a monoclinic phase nor any phase separation. Furthermore, the formation of the cubic spinel type Li_xCoO_2 reported in [3], usually badly affecting the battery performance, has not been detected either. Therefore, the real Li occupation ranges as $0.5 \leq x_{Li} \leq 1.0$ is expected, while Rietveld refinements yield $x_{Li} = 0.82(2)$ at 3.4 V and 0.17(2) at 4.2 V for the "fresh" cell. This difference becomes even more pronounced for the "fatigued" battery: i.e. 0.77(2) at 3.6 V and 0.09(2) at 4.2 V (see Fig. S3). A similar finding was already mentioned by Rodriguez et al. [12], where significant deviations between refined Li-occupations and those from inductively coupled plasma mass spectrometry were noticed. These authors have attributed the observed discrepancies to the weak penetration capability of X-rays, where most of signal is delivered from the relatively lithium-poor surface of the Li_xCoO_2 grain and not from the Li-rich core. However, this explanation cannot be used for neutron powder diffraction, where representative bulk properties are probed. In agreement with the reports of authors [2,3,12] the preferred orientation effects could affect an accurate determination of the Li content in cathode, but no significant texture for Li_xCoO_2 was evidenced from 2D diffraction data (Fig. S4). The origin of the observed discrepancy between refined and expected Li-occupation factors is not yet clear, obviously more detailed information needs to be extracted from an inclusion of amorphous parts in Li_xCoO_2 by complementary systematic *ex situ* examinations.

The effect of fatigue on the cathode side is rather weak and mainly concerns differences in the slope for Li occupation vs. voltage, although Li occupations are not very reliably quantified. Therefore no final conclusions can be drawn, but the following overall tendencies are derived from "*in-operando*" high resolution neutron powder diffraction: fatigue introduces changes in the slope of Li occupation vs. voltage, reflected a reduced amount of exchanged lithium during the intercalation process.

The Li intercalation into graphite takes place in stages, i.e. the formation of a periodic array of unoccupied layer gaps at low Li concentration occurs. Graphite can host a maximum of one Li per six C atoms, which corresponds to the LiC_6 composition (stage I). Other binary lithium intercalated graphites with less lithium amount are reported, e.g. LiC_{12} (stage II), LiC_{18} (stage IIL), LiC_{30} (stage III), etc. At low voltages only reflections consistent with hexagonal graphite are present. During charging an intercalation of lithium into carbon was observed (see Fig. S5) corresponding to the formation of LiC_{12} and LiC_6, respectively, which is reflected in the shift of the [0 0 2] graphite reflections due to the expansion of c-axis along with shift of the graphene layer against each other. Phases with lower lithium concentration, e.g. LiC_{18} and $LiC_{x\geq 25}$ [4] are expected to occur in the range of 3.6–3.9 V, which was not considered in detail in the current study. A closer inspection of the obtained diffraction data reveals a weak but systematic broadening of Bragg reflections for the Li-intercalated carbon phases in the case of the "fatigued" battery, which might indicate variations in microstructure or an inhomogeneous Li-distribution. Furthermore at 3.95 V, the phase fraction of LiC_6 for the "fresh" battery is obviously higher than those for the "fatigued" one (Fig. S5). This tendency continues at higher charging states, e.g. 4.00 V, 4.05 V, while at higher voltages ($\geq$4.10 V) the amount of LiC_6 in both "fresh" and "fatigued" batteries becomes nearly equal. As it is shown in Fig. 3 the LiC_{12} phase fraction for "fatigued" battery is systematically higher than the respective one in "fresh" cell, which occurs in cost of LiC_6 intercalated carbon, i.e. the LiC_6 phase fraction for "fatigued" cell is lower than that in the "fresh" cell at the same voltage. This fact unambiguously indicates less insertion of Li into the fatigued graphite anode.

More detailed information concerning the Li-ion battery design and its variations upon charging can be obtained from neutron radiography and tomography. This method has been already applied to studies of various technical devices and is an especially suitable tool for studies of Li-ion cells, since the neutrons have favourable properties with respect to mass attenuation in the various materials used [5,6,16]. The working principle of neutron radiography and tomography is well described [16,17]. In the present experiments both "fresh" and "fatigued" commercial Li-ion cells of 18650 type (18 mm diameter, 650 mm height) have been investigated and radiography images were collected at the tomography scanner ANTARES [18] for different battery rotations around

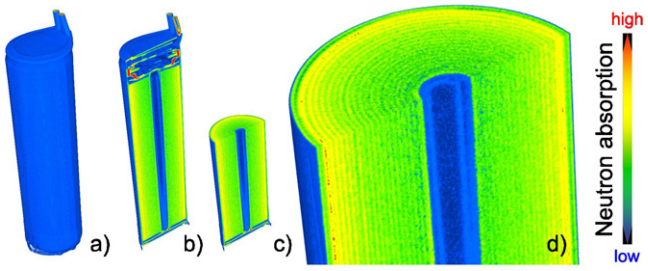

Fig. 4. 3D model of commercial 18650 Li-ion battery reconstructed from neutron radiography (a), its vertical cut (b), its vertical and horizontal cut (c) and its enlarged view (d). Absorption levels are visualized by assignment to different colours.

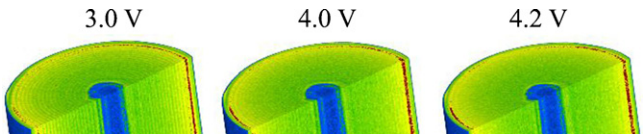

Fig. 5. Slices of 3D models for commercial 18650 Li-ion battery charged to 3.00 V (a), 4.00 V (b) and 4.20 V (c) as reconstructed from neutron radiography.

the cylinder axis with an exposure time of 60 s and an overall field of view of 100 mm × 100 mm. In combination with the high collimation ratio (L/D = 800) a pixel resolution of about 100 μm was achieved. The 3D reconstruction was performed on the basis of a batch consisting of 600 single projections using a filtered back projection algorithm. Data visualization was done with VGStudio Max from Volume Graphics [19].

The results of the 3D reconstruction are shown in Fig. 4a in false-colour representation. The resolution of this neutron tomography setup was sufficient to resolve the steel can, gasket, safety vent and circuits inside a Li-ion battery (Fig. 4b) as well as cathode/anode layers rolled around the Cu-sword (Fig. 4c). An enlarged view of Fig. 4c is shown in Fig. 4d and points out an absorption gradient from the centre (green colour) towards the outer region (yellow colour), which corresponds to an increase of the local neutron absorption capability. As the natural isotope composition for Li is 7.5% of ^{6}Li and 92.5% of ^{7}Li, where ^{6}Li has a very high absorption cross section, the observed absorption gradient can be attributed to the distribution of lithium inside the battery, i.e. more lithium is concentrated in the outer part of the battery. Comparison of data collected for "fresh" and "fatigued" lithium cells showed their visual identity, so that 200 steps of charge/discharge do not cause significant changes on a macroscopic level.

Neutron radiography studies performed at different charging states (3.00, 4.00 and 4.20 V) resulted in a different contrast between cathode and anode layers, e.g. well resolved cathode and anode layer boundaries at 3.00 V, but significantly smeared out ones at 4.20 V (see Fig. 5). A derivative analysis of the observed tomography images requires more sophisticated analysis due to changes in the battery dimensions upon charging/discharging from 3.0 V to 4.2 V (ca. 55 μm in diameter). The smearing out of the cathode/anode layer boundaries at elevated charge levels reflects the more homogeneous Li distribution then in the discharged states, i.e. all lithium is in the cathode and in the electrolyte, while the anode is nearly Li free (except solid-electrolyte interface and soaked electrolyte).

The performed studies unambiguously emphasize the need of neutron scattering for the investigations to address the serious challenges in Li-ion battery technology which still remain unanswered. A more clear understanding of these effects can be obtained from supplementary neutron scattering experiments at non-ambient conditions, which allow following the degradation "live" during operation.

Acknowledgment

This work was supported by Deutsche Forschungsgemeinschaft (Research Collaborative Centre 595 "Electrical Fatigue in Functional Materials").

Appendix A. Supplementary data

Supplementary data associated with this article can be found, in the online version, at doi:10.1016/j.jpowsour.2011.12.007.

References

[1] M.A. Rodriguez, D. Ingersoll, S.C. Vogel, D.J. Williams, Electrochem. Sol. State Lett. 7 (1) (2004) A8–A10.
[2] M.A. Rodriguez, M.H. van Benthem, D. Ingersoll, S.C. Vogel, H.M. Reiche, Powder Diffr. 25 (2) (2010) 143–147.
[3] N. Sharma, V.K. Peterson, M.M. Elcombe, M. Avdeev, A.J. Studer, N. Blagojevic, R. Yusoff, N. Kamrulzaman, J. Power Sources 195 (2010) 8258–8266.
[4] L. Liang, S.S. Lee, H.S. Choi, B.-S. Seong, C.-W. Yi, K. Kim, 216th Meeting of Electrochemical Society, 4–9 October 2009, Vienna, Austria, Conference Abstracts 902 (8) (2009) 549.
[5] M. Kamata, T. Esaka, S. Fujine, K. Yoneda, K. Kanda, J. Power Sources 68 (1997) 459–462.
[6] M. Lanz, E. Lehmann, R. Imhof, I. Exnart, P. Novak, J. Power Sources 101 (2001) 177–181.
[7] D. Goers, M. Holzapfel, W. Scheifele, E. Lehmann, P. Vontobel, P. Novak, J. Power Sources 130 (2004) 221–226.
[8] I. Manke, J. Banhart, A. Haibel, A. Rack, S. Zabler, N. Kardjilov, A. Hilger, A. Melzer, H. Riesemeier, Appl. Phys. Lett. 90 (2007) 214102.
[9] M. Hoelzel, A. Senyshyn, N. Juenke, H. Boysen, W. Schmahl, H. Fuess, Nucl. Instr. Meth. A 667 (2012) 32–37.
[10] T. Roisnel, J. Rodriguez-Carvajal, Mater. Sci. Forum 378–381 (2001) 118–123.
[11] G.G. Amatucci, J.M. Tarascon, L.C. Klein, J. Electrochem. Soc. 143 (1996) 1114–1123.
[12] M.A. Rodriguez, D. Ingersoll, D.H. Doughty, JCPDS Advances in X-ray analysis 45 (2002) 182–187.
[13] J.N. Reimers, J.R. Dahn, J. Electrochem. Soc. 139 (1992) 2091–2097.
[14] T. Ohzuku, A. Ueda, J. Electrochem. Soc. 141 (1994) 2972–2977.
[15] M. Inaba, Y. Iriyama, Z. Ogumi, Y. Todzuka, A. Tasaka, J. Raman Spectrosc. 28 (1997) 613–617.
[16] J.C. Domanus (Ed.), Practical Neutron Radiography, Kluwer Academic Publishers, Dodrecht, the Netherlands, 1992.
[17] J. Banhart (Ed.), Advanced Tomographic Methods in Materials Research and Engineering, Oxford University Press, Oxford, UK, 2008.
[18] http://einrichtungen.physik.tu-muenchen.de/antares/.
[19] http://www.volumegraphics.com/products/vgstudiomax/.